

The Influence of Silicon on the Corrosion Behavior
of AISI 304 Stainless Steels

C.S. Machado
Department of Materials
Instituto de Pesquisas Energeticas e Nucleares
C.P. 11049, Cidade Universitaria
05508 Sao Paulo
Brazil

L.V. Ramanathan
Department of Materials
Instituto de Pesquisas Energeticas e Nucleares
C.P. 11049, Cidade Universitaria
05508 Sao Paulo
Brazil

Conquistado
CORROSION-Asia
Singapore
Set '92

IPEN-DOC- 1987

COLEÇÃO PTC

DEVOLVER AO BALCÃO DE EMPRÉSTIMO

Abstract

The influence of adding upto 4.7wt% Si to AISI 304 on the general corrosion resistance in H_2SO_4 , and pitting as well as intergranular corrosion resistance has been studied. The alloys were prepared by melting in a vacuum induction furnace and annealed at 1200 C for 2 hours followed by quenching. Anodic polarization tests of the alloys in 1N H_2SO_4 revealed that the critical current density decreased with increasing Si upto 2.5wt% and thereafter increased again. Prolonged immersion tests in $FeCl_3$ and anodic polarization measurements in 3.5% NaCl revealed that with increasing Si the tendency of the alloy to pit decreased and the pitting potential increased. The susceptibility to intergranular corrosion as determined through Huey tests also decreased with Si content. The overall influence of Si in the alloy on the corrosion behavior is considered to be due to incorporation of Si in the surface film and consequent improvement in adhesion as well as reduction in defects within the film.

Introduction

Austenitic stainless steels (SS) have been widely used due to their excellent mechanical properties and resistance to general aqueous corrosion. They are however susceptible to various forms of localized corrosion such as pitting, crevice and intergranular (i.g.) corrosion. These forms of localized corrosion depend on both environmental factors such as aggressive ion concentration, temperature, agitation etc. as well as alloy related factors such as composition, microstructure, precipitated phases etc. The presence of small quantities of ferrite in austenitic stainless steels has been reported to be deleterious in terms of the localized corrosion behavior. On the other hand, duplex stainless steels with high ferrite content exhibit improved corrosion resistance (1). The addition of certain elements such as Si, Mo, V to austenitic SS stabilizes the ferrite phase and it has been shown that these elements reduce pitting susceptibility (1-3). Wilde found that the addition of upto 4.5% Si to Fe18Cr8Ni SS increased pit initiation resistance by a factor of 20 and crevice

corrosion susceptibility to be adversely affected (4). In terms of i.g. corrosion susceptibility, the ferrite phase was found to be beneficial (5). In the presence of Si, significant increase in i.g. corrosion resistance of annealed alloys has been reported (6). In order to extend information about the effect of Si addition, and consequently the δ ferrite phase on the corrosion behavior of SS, the influence of adding 0-5wt% Si to AISI 304 on the general, pitting, crevice and intergranular corrosion behavior has been reported.

Materials and Methods.

AISI 304 was vacuum induction melted and Si added to it to obtain the 5 alloys with compositions as shown in Table I. Specimens obtained from the alloy ingots were annealed at 1200 C for 2hs followed by a water quench. Optical microscopic examination of the specimens was carried out following standard metallographic preparation.

Table I. Chemical composition of experimental alloys.

Alloy	Chemical composition (wt%)										
	C	Mn	P	S	Cr	Ni	Mo	N ppm	Ti	Si	δ ferrite %
1	0.068	1.38	0.033	0.008	18.23	8.16	0.04	524	0.002	0.62	5.83
2	0.07	1.39	0.019	0.008	19.3	9.0	0.09	532	0.002	0.92	9.90
3	0.067	1.52	0.017	0.007	19.1	9.6	0.09	550	0.003	1.51	10.1
4	0.069	1.53	0.019	0.009	18.9	9.4	0.09	512	0.002	2.46	13.5
5	0.068	1.55	0.02	0.008	18.6	9.1	0.1	521	0.002	4.73	26.00

The corrosion tests consisted of (a) anodic potentiodynamic polarization measurements in 1N H_2SO_4 and 3.5wt% NaCl. The alloys were polarized in the range -500 mV to +1100 mV (vs SCE) at 10mV/s, (b) immersion for 96 hours in 10% $FeCl_3$ solution at 25 C and (c) standard Huey tests in boiling 65% HNO_3 for 48 hours following an initial screening test in oxalic acid. Potentiodynamic reverse scans from -100mV to +1000mV to -100mV were also carried out and the repassivation potential E_{rp} read out from the curves. The difference $E_p - E_{rp}$ for the different alloys was obtained to determine the extent of susceptibility to crevice corrosion (4).

Results and Discussions

The δ ferrite content of the alloys as determined from Shaefflers diagram are shown in Table I. and it can be seen that the ferrite content increased with Si in the alloy. Optical microscopic examination of the annealed specimens revealed that Alloy 1 had an

all austenite structure (fig.1). Comparison of the structures of Alloys 2-4 shows that with increasing Si, the ferrite grains increased in size from being spots to large coalesced particles. Alloy 5 had an all ferrite structure with a fine distribution of carbides. This structure results because the position of this alloy at the annealing temperature in the phase diagram shifts to the single phase ferrite field and this phase is retained upon quenching. The fine carbides in the ferrite matrix result due to the low solubility of C in δ ferrite.

Anodic potentiodynamic polarisation measurements in 1N H_2SO_4 revealed that the passivation potential was $\sim -300mV$ and the critical current density decreased with increasing Si in the range 0 to 2.5% but increased thereafter with Si upto 4.7wt% as shown in Table II.

Table II. Influence of Si on the electrochemical parameters of Si containing AISI 304 in 1N H_2SO_4 .

Alloy	1	2	3	4	5
Ep(mV)	-306	-306	-292	-308	-301
i.crit($\mu A/mm^2$)	15.62	13.78	10.51	8.62	12.11

The anodic polarization curves of the alloys in 3.5% NaCl are shown in figure 2. It can be seen that the pitting potential E_p increased with Si content of the alloys. The pitting corrosion rates of the different alloys as determined from the $FeCl_3$ immersion tests are shown in figure 3. The pitting rate decreased with Si content and this decrease is more pronounced as the solution volume to specimen area ratio increased. The extent to which pitting rate decreased with Si content upto 4.5wt% although significant, is not as high as reported elsewhere (4). The low corrosion rates at low solution volume to specimen area ratios may be attributed to early saturation of the solution with complexed metal chlorides. The results of the optical microscopic examination of the pitted surfaces are summarized in Table III.

Table III. Pitted surface features following prolonged immersion in $FeCl_3$.

Alloy	Description
1	Various large pits 1-3mm close to each other forming craters and fine pits over rest of the surface.
2	Various large pits (1-3mm) and some very fine pits.
3	Some medium sized pits (1-2mm) and few small pits.
4	Some medium sized pits (1-2mm) and few small pits.
5	Very few small pits (0.5-1mm).

The initial oxalic acid screening test revealed that alloys 1 to 4 in the annealed state were not susceptible to i.g. corrosion. Alloy 5 was severely corroded in both the oxalic acid test and the Huey test and this could be attributed to the Cr depleted zones resulting from $M_{23}C_6$ precipitation at the ferrite matrix. Upon sensitizing the alloys at 600 C for 20 hours it was noticed that all the alloys were susceptible to i.g. corrosion, although the rate decreased with increasing Si content as shown in Table IV.

Table IV. Intergranular corrosion behavior of alloys as determined by Huey test. Corrosion rate in mmpy.

Alloy	1	2	3	4	5
Annealed	-	-	-	-	1.21
Sensitized 600C - 20h	1.44	0,77	0.16	0.21	0.56

From the anodic polarization curves of the alloys in the 3.5% NaCl, the values of E_p , E_{rp} and $(E_p - E_{rp})$ were computed as shown in Table V. The $(E_p - E_{rp})$ considered to be indicative of the possible extent of crevice corrosion increases with Si content of the alloy. These observations were found to be in agreement with data reported in (4).

Table V. Pitting and repassivation potentials of the alloys in aerated 3.5% NaCl. Scan rate 10mV/s

Alloy	Pitting potential (mV) E_p	Repassivation potential (mV) E_r	$E_p - E_r$ (mV)
1	221	-10	231
2	252	-29	281
3	405	-20	425
4	476	-10	486
5	1000	---	---

General discussions

The equilibrium structure of the matrix phase of Alloy 1 below 1200 C is austenitic and that of the Si containing alloys austenite and ferrite. The amount of δ ferrite in the alloys increased with Si content. In chloride ion containing environments all the alloys pitted, although the pitting potential, the extent of the pitting and the pit nucleation sites varied with alloys composition. Pits were observed in the γ as well as the δ phase as observed from SEM/EDAX studies (fig.4). The pitting potential increased with Si content of the alloys. Since pitting occurs at sites where the passive film is

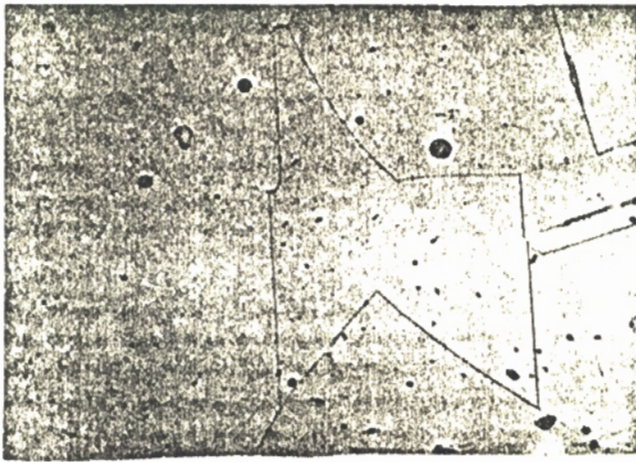
ruptured by the aggressive Cl^- ions, the higher E_p of the Si containing alloys can be attributed to the formation of a more continuous and nearly defect free film of Cr_2O_3 and SiO_2 on the ferrite phase. The i.g. corrosion resistance of the Si containing alloys is not altered by the presence of the ferrite phase. However heat treatment in the sensitizing zone results in carbide precipitation, consequent formation of Cr depleted zone and increased susceptibility. Nevertheless the presence of Si decreases the i.g. corrosion susceptibility considerably as compared to the Si free alloy.

Conclusions

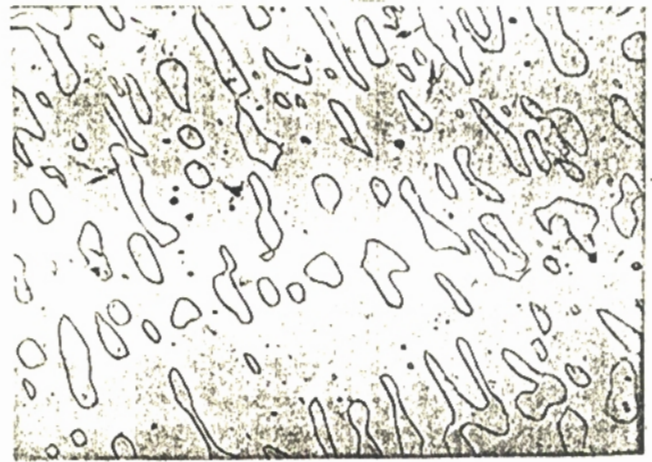
1. The addition of upto 4.5wt% Si to AISI 304 increases the δ ferrite content upto 26%.
2. In chloride ion containing solutions, the extent of pitting decreases with increasing Si content. The pitting potential increased with Si content.
3. In the annealed state, the alloys are not susceptible to i.g. corrosion, whereas in the sensitized state all the alloys become susceptible. However the extent of i.g. corrosion of the sensitized alloys decrease with the increasing Si content.

References

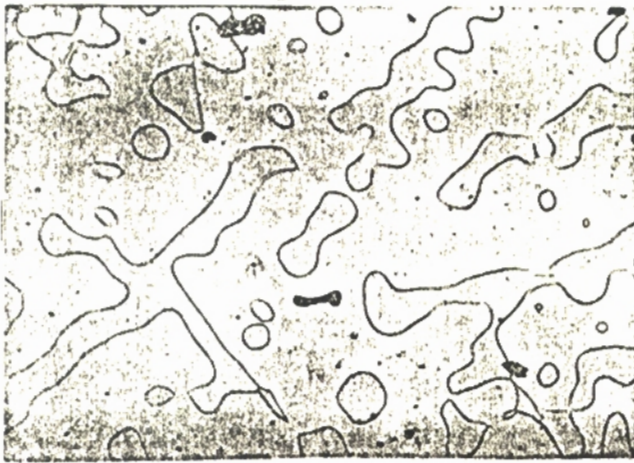
1. Sedriks, A.J. Corrosion of Stainless Steels, John Wiley and Sons, Inc, New York, NY, 1979.
2. Tomashov, N.D., Chernova, O.P., and Markova, O.N., Corrosion, vol.20, 5, 1964, 166t.
3. Truman, J.E., "Corrosion, Metal/Environment Reactions," Shreir, L.L., Ed., Vol.1, Newnes Butterworths, London, 1976, 331.
4. Wilde, B.E., Corrosion, 42, 3, 1986, 147.
5. Wilde, B.E., Weber, J.E., Brit. Corros. J., 4, 1969, 42.
6. Wilde, B.E., Corrosion, 44, 10, 1988, 699.



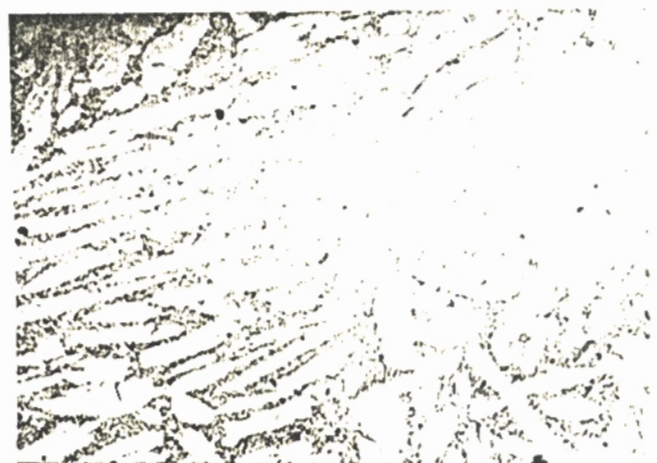
(a)



(b)



(c)



(d)



(e)

Figure 1. Optical micrographs of annealed alloys. (a) Alloy 1, (b) Alloy 2, (c) Alloy 3, (d) Alloy 4, (e) Alloy 5. 200X.

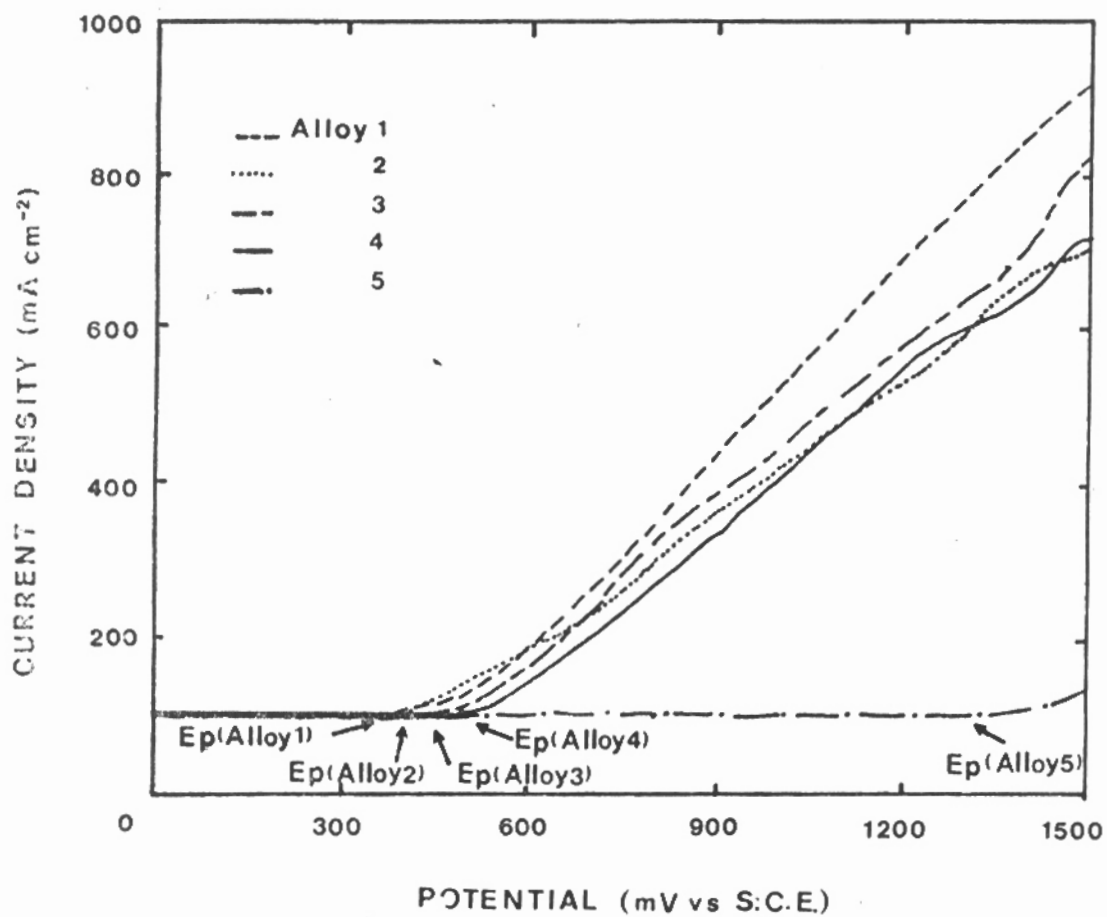


Figure 2. Anodic polarization curves of Si containing stainless steels in 3.5% NaCl at 25 C.

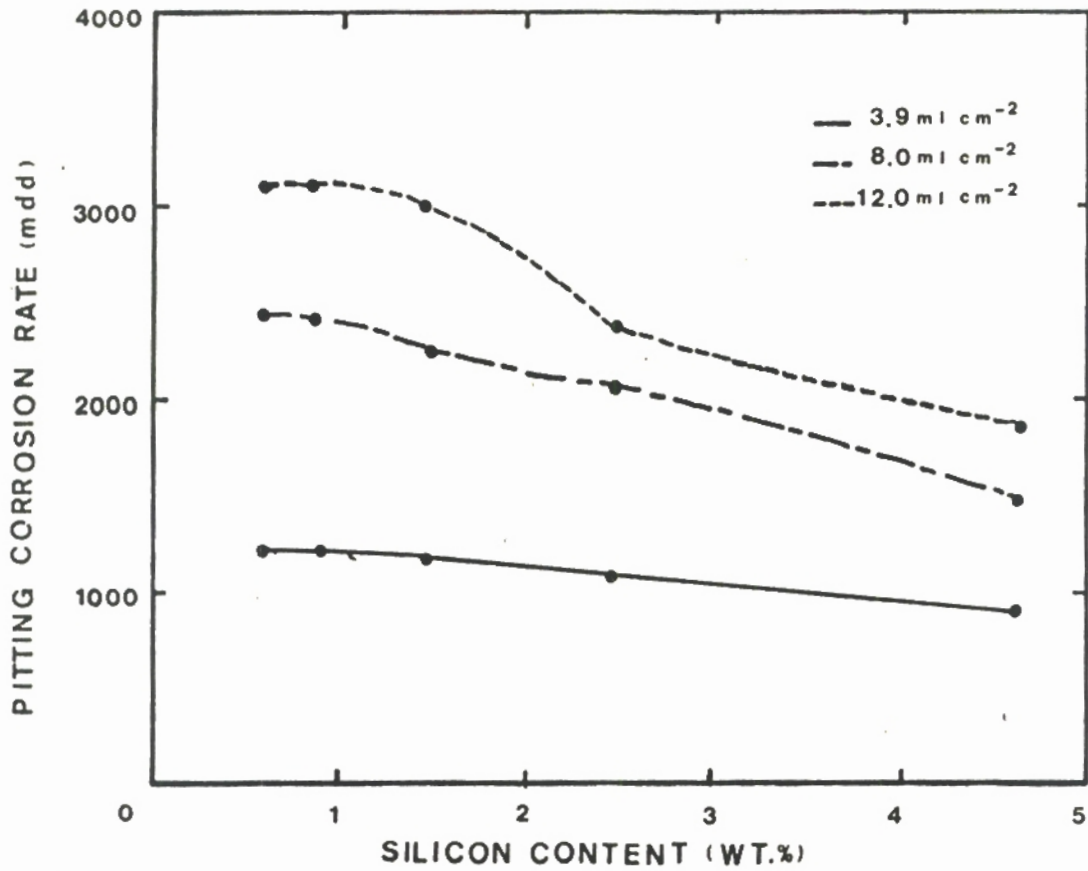


Figure 3. Pitting corrosion rate in 10% ferric chloride as a function of Si content in AISI 304 stainless steels.

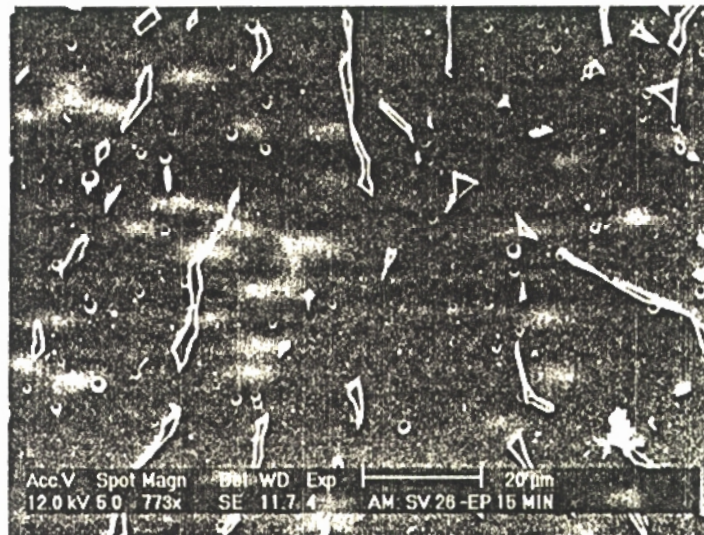


Figure 4. Scanning electron micrograph of Alloy 4 polarized in 3.5% NaCl at E_p for 15 minutes.